



ELSEVIER

Contents lists available at ScienceDirect

## Continental Shelf Research

journal homepage: [www.elsevier.com/locate/csr](http://www.elsevier.com/locate/csr)

## Research Papers

## Seasonal variability of chlorophyll a in the Mid-Atlantic Bight

Yi Xu<sup>a</sup>, Robert Chant<sup>a</sup>, Donglai Gong<sup>a</sup>, Renato Castelao<sup>b</sup>, Scott Glenn<sup>a</sup>, Oscar Schofield<sup>a,\*</sup><sup>a</sup> Coastal Ocean Observation Lab, Institute of Marine and Coastal Sciences, School of Environmental and Biological Sciences, Rutgers University, New Brunswick, NJ, 08901, USA<sup>b</sup> Department of Marine Science, University of Georgia, Athens, GA, 30602, USA

## ARTICLE INFO

## Article history:

Received 9 June 2010

Received in revised form

13 May 2011

Accepted 31 May 2011

## Keywords:

Ocean color

Phytoplankton

Mid-Atlantic Bight

## ABSTRACT

For this manuscript we use a 9-year time series of Sea-viewing Wide Field of view Sensor (SeaWiFS), HF radar, and Webb Glider data to assess the physical forcing of the seasonal and inter-annual variability of the spatial distribution in phytoplankton. Using Empirical Orthogonal Function (EOF) analysis, based on 4-day average chlorophyll composites, we characterized the two major periods of enhanced chlorophyll biomass for the MAB in the fall–winter and the spring. Monthly averaged data showed a recurrent chlorophyll biomass in the fall–winter months, which represented 58% of the annual surface chlorophyll for the MAB. The first EOF mode explained ~33% of the chlorophyll variance and was associated with the enhanced phytoplankton biomass in the fall–winter found between the 20 and 60 m isobaths. Variability in the magnitude of the enhanced chlorophyll in fall–winter was associated with buoyant plumes and the frequency of storms. The second EOF mode accounted for 8% of the variance and was associated with the spring time enhancements in chlorophyll at the shelf-break/slope (water depths greater than 80 m), which was influenced by factors determining the overall water column stability. Therefore the timing and the inter-annual magnitude of both events are regulated by factors influencing the stability of the water column, which determines the degree that phytoplankton are light-limited. Decadal changes observed in atmospheric forcing and ocean conditions on the MAB have the potential to influence these phytoplankton dynamics.

© 2011 Elsevier Ltd. All rights reserved.

## 1. Introduction

The Mid-Atlantic Bight (MAB) is a biologically productive continental shelf that is characterized by consistently high chlorophyll biomass ( $> 1 \text{ mg chlorophyll m}^{-3}$ ), which supports a diverse food web that includes abundant fin and shellfish populations (Yoder et al., 2001). The MAB's shelf extends out for several hundred kilometers and the associated water mass is bounded offshore by the shelf-break front. While the shelf-break front is often near the geological shelf-break, the surface outcrop of the front can extend beyond the continental slope (Wirick, 1994). In the nearshore regions there are numerous inputs from moderately sized, yet heavily urbanized, rivers (Hudson River and Delaware River), which are sources of fresh water, nutrients, and organic carbon to the MAB (O'Reilly and Busch, 1984). The waters on the MAB exhibit considerable seasonal and inter-annual variability in temperature and salinity (Mountain, 2003). In late spring and early summer, a strong thermocline (water temperatures can span from 30 to 8 °C in  $< 5 \text{ m}$ ) develops at about the 20 m depth across the entire shelf, isolating a continuous mid-shelf "cold pool" (formed in winter

months) that extends from Nantucket to Cape Hatteras (Houghton et al., 1982; Biscaye et al., 1994). The cold pool persists throughout the summer until fall when the water column overturns and mixes in the fall (Houghton et al., 1982), which presumably replenishes nutrients to the surface waters on the MAB shelf. Thermal stratification re-develops in spring as the frequency of winter storms decrease and surface heat flux increases (Lentz et al., 2003).

In temperate seas, seasonal phytoplankton variability has been related to stratification, destratification, and incident solar irradiance (Cushing, 1975; Longhurst, 1998; Dutkiewicz et al., 2001; Ueyama and Monger, 2005). During late winter and early spring, increasing solar illumination combined with decreasing wind result in shallower surface mixed layers, which allows for increased phytoplankton growth prior to the development of the thermal stratification (Stramska and Dickey, 1994; Townsend et al., 1994). As the physical regulation of water column turnover is spatially variable along the MAB, the temporal patterns in phytoplankton biomass are not always spatially coherent within the East Coast shelf/slope ecosystem (Yoder et al., 2001). While it has long been appreciated that seasonal phytoplankton blooms are important in shelf and slope waters of the MAB (Riley, 1946, 1947; Ryther and Yentsch, 1958), a 7.5-year (October 1978–July 1986) time series of the coastal zone color scanner (CZCS) imagery found that the maximum chlorophyll concentration appeared during

\* Corresponding author. Tel.: +1 732 932 6555; fax: +1 732 932 8578.

E-mail address: [oscar@marine.rutgers.edu](mailto:oscar@marine.rutgers.edu) (O. Schofield).

fall–winter on the continental shelf waters and that slope waters possessed a secondary spring peak in addition to the fall–winter bloom (Yoder et al., 2001). Ryan et al. (1999) used CZCS imagery from 1979 to 1986 and found an annual enhancement of chlorophyll at the shelf-break of the MAB and Georges Bank during the spring transition from well-mixed to stratified conditions. The shelf-edge system was similar to inner shelf waters in terms of seasonal heating and cooling; however, meanders at the shelf slope were associated with iso-pycnal upwelling that supplied nutrients to the euphotic zone and enhanced chlorophyll biomass (Ryan et al., 1999). Despite past efforts, understanding what regulates the magnitude of these seasonal patterns remains an open question, which is especially important as the MAB has experienced significant changes in water properties over the last few decades (Mountain, 2003).

Many factors are known to regulate the upper mixed layer dynamics on the MAB. These features include wind driven mixing (Beardsley et al., 1985) as well as surface buoyant plumes that frequently extend over significant fractions of the MAB shelf (Castelao et al., 2008a; Chant et al., 2008a). These features are superimposed upon the seasonal warming that drives the stratification of the MAB. This seasonality of shelf stratification regulates the phasing and potential magnitude of the fall–winter and spring enhancements in chlorophyll concentration. For this manuscript we use a 9-year time series of Sea-viewing Wide Field of view Sensor (SeaWiFS), HF radar, and Webb Glider data to assess the physical forcing of the seasonal and inter-annual variability of the spatial distribution in phytoplankton.

## 2. Methods

### 2.1. Ocean color remote sensing data

Time series of surface chlorophyll concentration in the MAB was studied using 4-day averaged composites of SeaWiFS satellite imagery collected from January 1998 to December 2006. We used 4-day average composites as they provided reasonable coverage for our study site and could resolve the dynamics of the chlorophyll over both seasonal and higher frequency scales (days to weeks) often observed in MAB. The 4-day average decreased the cloud contamination that heavily degraded the utility of the 1-day images. Many phytoplankton bloom events occur over time scales much shorter than a month in these waters. For example chlorophyll associated with buoyant plume events can last for the time scale of 4–5 days (Schofield et al., submitted for publication) and summer upwelling on average lasts for < 7 days in the MAB (Glenn et al., 2004). Longer term averaging underemphasizes these shorter-lived phytoplankton bloom events that can explain up to 44% of the variability observed in daily satellite imagery (Yoder et al., 2001). The spatial resolution of the original images were 1.1 km, however, data were re-gridded to 5.5 km in order to identify the principal modes of variability in the data set by Empirical Orthogonal Function (EOF) analysis. Given the high spatial heterogeneity in the nearshore waters and the increasing error in satellite estimates of chlorophyll in shallow waters, we excluded regions with water depths shallower than 10 m for this analysis. We also excluded data for water depths deeper than 2000 m, as our focus was on the shelf and shelf-break region. Finally we excluded data from large inland Bays (Long Island Sound, Delaware Bay and Chesapeake Bay; Fig. 1). Monthly chlorophyll concentration was calculated by taking the geometric mean at each pixel. We chose to use the geometric rather than the arithmetic mean because the distribution of chlorophyll measurements in continental shelf and slope waters is approximated by a log-normal distribution (Campbell, 1995; Yoder et al., 2001).

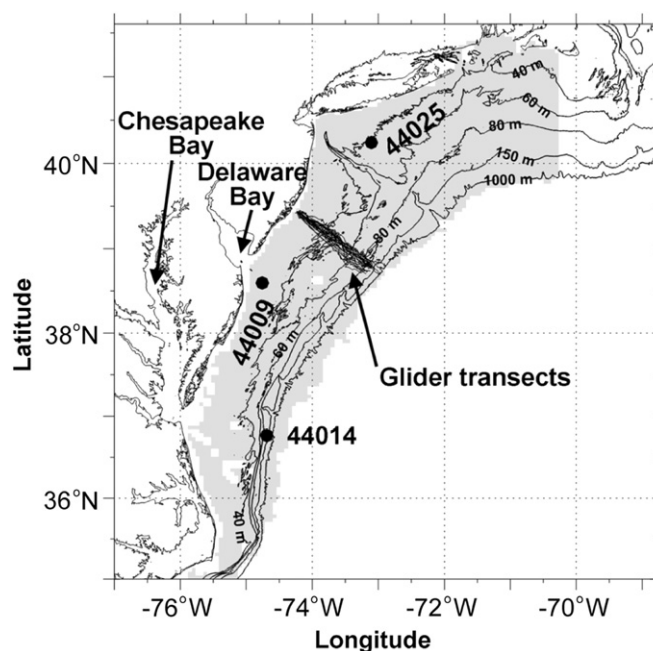


Fig. 1. Map showing study area, NDBC mooring stations, and glider tracks. Topographic contours shown are 40, 60, 80, 150, and 1000 m. Gray shaded area indicates region where SeaWiFS imagery was analyzed.

Ocean color satellite remote sensing has limitations in coastal waters. Satellite coverage is limited by cloud cover especially in the winter months, which is characterized by frequent storms. Storms also can produce buoyant plumes that contain significant amounts of sediment and colored dissolved organic matter. The presence sediment and CDOM can influence the accuracy of the satellite-derived estimates of chlorophyll that can result in errors as large as 50–100% in the nearshore waters of the northeast United States (Harding et al., 2004). Finally, ocean color remote sensing does not provide information on subsurface phytoplankton peaks, below the detection limit of the satellite, which are often present in the MAB. While we acknowledge these shortcomings, satellite estimates of chlorophyll remains one of the only techniques that can provide decadal spatial time series over ecologically relevant scales.

We also calculated the monthly climatological sea surface temperature (SST) for each pixel based on 4-day averaged Advanced Very High-Resolution Radiometer (AVHRR) data sets from 1999 to 2006. The AVHRR data sets were collected by a satellite dish maintained by Rutgers University Coastal Ocean Observation Lab and processed using SeaSpace AVHRR processing software. Monthly SeaWiFS Level 3 photosynthetically available radiation (PAR) data from 1998 to 2006 were downloaded from <http://oceancolor.gsfc.nasa.gov>. The PAR data sets have the resolution of 9 km and the climatology of PAR was calculated based on the 9-year monthly data sets.

The mean satellite-derived chlorophyll fields were used as inputs to the Hydrolight 4.3 radiative transfer model (Mobley, 1994) to estimate the depth of the 1% light levels. For the Hydrolight simulations, we used default settings and assumed a constant backscatter to total scatter ratio of 0.05 based on data collected in this region (Moline et al., 2008). We assumed there was no inelastic scattering and kept wind speeds at zero. The surface flux of light was calculated using a semi-empirical sky model (Mobley, 1994) for the MAB at local noon on a cloudless day. We assumed that water column was infinitely deep. These Hydrolight simulations assumed no vertical structure in the phytoplankton biomass. We used this approach even though

during the stratified season there can be subsurface chlorophyll layers however, satellite-derived chlorophyll estimates were used as the input to the Hydrolight simulation and these estimates are exponentially weighted to the surface waters (Mobley, 1994); therefore it is unlikely that satellite estimates included any significant proportion of the subsurface populations found at the base of the pycnocline in the late spring and summer months. Given this we did not impose a vertical structure for chlorophyll. For these simulations we treated the MAB as Case I waters (Johnson et al., 2003). This assumption is sometimes not the case when the Hudson River carries significant amounts of detritus and colored dissolved organic matter (CDOM) offshore onto the MAB (Johnson et al., 2003). Despite the optical complexity of these waters, SeaWiFS can accurately and reliably capture seasonal and inter-annual variability of chlorophyll *a* associated with variations of fresh water flow (Harding et al., 2004), which can increase chlorophyll biomass by an order of magnitude. To assess the impact of Case II conditions on our Hydrolight estimates of the 1% light depth, we used optical data collected as part of the LaTTE experiment (Chant et al., 2008b), which in part focused on characterizing the optical properties of the Hudson River waters being transported out onto the MAB (Moline et al., 2008). During the LaTTE experiment, data were collected from the Hudson River outflow over time with a WETLabs, Inc. absorption/attenuation meter using the methods outlined in Schofield et al. (2004). The waters were influenced by the Hudson River, which was characterized by significant contributions of chlorophyll and CDOM providing Case II waters. These measurements of the optical properties were inputted into the Hydrolight model to provide an estimate for light propagation in the Case II characteristics for MAB waters.

## 2.2. Winds and surface current observations

Wind data were obtained from moored buoys deployed by the National Data Buoy Center (NDBC) (<http://www.ndbc.noaa.gov/maps/Northeast.shtml>). We used data collected by mooring 44025 (Fig. 1) located at 40.25°N, 73.17°W with a water depth of 36 m and mooring 44014 (Fig. 1) located at 36.61°N, 74.84°W with a water depth of 48 m. The reason we chose these two moorings was because 44025 was located at the mid-shelf region while 44014 was located at shelf-break/slope region. We used the daily wind speed data to calculate the stormy frequency. The wind data used for calculating the correlation coefficient between the surface currents measured by CODAR and wind speed were based on the time series of the 6 years (2002–2007) wind measured at NDBC 44009 (Fig. 1) located at 38.46°N, 74.70°W with a water depth of 28 m. We used this mooring as it was central to a recently completed long-term analysis of the circulation on the MAB (Gong et al., 2010). The wind data for 44009 were decomposed into along-shelf and cross-shelf directions (30 degree rotation) and low-passed with a 33-hour filter. Shore-based High Frequency (HF) radar systems were used for surface current measurements. The radar network was a fully nested array of surface current mapping radars (Kohut and Glenn, 2003; Kohut et al., 2004). Hourly surface currents were measured with an array of CODAR HF Radar systems consisting of 6 long-range (5 MHz) and 2 high-resolution (25 MHz) backscatter systems from the start of 2002 to the end of 2007. For all systems measured beam patterns were used in surface current estimates (Kohut and Glenn, 2003). Details of HF radar development and theory can be found in Crombie (1955), Barrick (1972), Stewart and Joy (1974), Barrick et al. (1977). All CODAR surface currents were de-tided using the T\_TIDE Matlab package (Pawlowicz et al., 2002) before further analysis is performed. The averaged seasonal surface current responses for the dominant winds were calculated

for the well-mixed winter (December–March), the transitional seasons (April–May, October–November), and stratified summer (June–September; Gong et al., 2010).

## 2.3. River discharge and glider data

The monthly river discharge data were downloaded from <http://nwis.waterdata.usgs.gov/nwis>. The total river discharge into to the MAB was represented by the sum of the discharges from Mohawk River at Cohoes, NY (42.79°N, 73.71°W), Passaic River at Little Falls, NJ (40.89°N, 74.23°W), Raritan River below Calco Dam at Bound Brook, NJ (40.55°N, 74.55°W), Hudson River at Fort Edward, NY (43.27°N, 73.60°W), and Delaware River at Trenton, NJ (40.22°N, 74.78°W).

Webb Slocum gliders were used to obtain subsurface measurements over the shelf. The Webb gliders occupy a cross-shore transect across the MAB beginning in 2005 (Schofield et al., 2007); however, the coverage in each month is not always complete. The cross-shelf transects typically take on average 4–5 days and are appropriate for comparing to the 4-day averaged satellite imagery. The cross-shore transect typically spans the 15–100 m isobaths (Fig. 1). The gliders were outfitted with CTDs (Sea-Bird Electronics, Inc.) and occasionally with optical backscatter sensors (WETLabs, Inc.). For this effort we were able to utilize the data collected from 19 cross-shore transects; however, the coverage was not uniform over the year. There were 7 transects available during the fall and winter; however, many of the early transects consisted of a glider that was not outfitted with a fluorometer or a backscatter sensor. Only 2 of 7 transects in fall and winter had any optical sensors present on board. Unfortunately no fluorometry data is available for the winter season and only one transect had only partial data of optical backscatter. There were twelve transects that were available for both the spring and summer and all the gliders were outfitted with optical backscatter and chlorophyll fluorometers. We compared individual transects and to specific satellite imagery and also averaged the glider observations (Castelao et al., 2008b). While the glider data were sparser than the satellite and CODAR data, it represented the densest concurrent subsurface data available for the MAB.

## 2.4. EOF and cluster analysis

EOF analysis is the mapping of the multi-dimensional data sets onto a series of orthonormal functions and is useful in compressing the spatial and temporal variability of large data sets down to the most energetic and coherent statistical modes. EOF results can be quite informative; however, they do not necessarily demonstrate causality and should be interpreted with caution. This method was first applied by Lorenz (1956) to develop the technique for statistical weather prediction. These approaches have been extremely useful for analyzing ocean color images, which have long time series and significant spatial variability (Baldacci et al., 2001; Yoder et al., 2001; Brickley and Thomas, 2004; Navarro and Ruiz, 2006). As EOF requires data sets without spatial gaps, we only used images that had less than 20% of pixels removed because of clouds. Additionally, prior to performing EOF analysis, any gaps in the data, due to clouds, were replaced by the average of the surrounding 8 non-cloud pixels. Using the criteria of less than 20% cloud cover, our final data set resulted in total of 468 4-day composites images with sufficient temporal resolution to resolve short-lived chlorophyll events. The numbers of images in each month used in the EOF analysis are presented in Fig. 2. EOF analysis was performed after subtracting the temporal mean of each pixel over the entire time series.

Additionally, we analyzed the chlorophyll variability using a cluster analysis. This was used to access to what degree the different

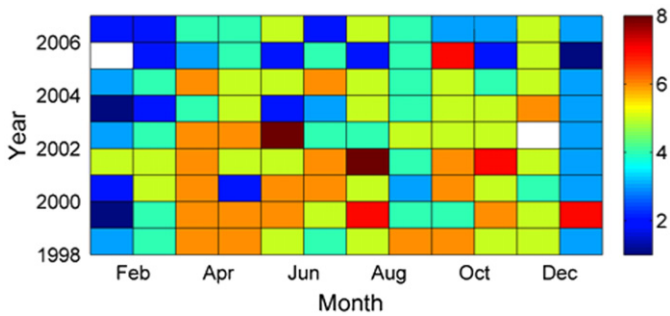


Fig. 2. Number of images used each month for the entire time series of 4-day chlorophyll composites.

environmental conditions were associated with the chlorophyll concentrations over the 9-year data sets. Cluster analysis was carried out using Ward's method to minimize the sum of the squares of any two hypothetical clusters that can be formed at each step (Ward, 1963) in order to emphasize the homogeneous nature of each cluster. The cluster analysis was conducted using storm frequency, maximum chlorophyll concentration and mean river discharge during winter time (Dec.–Jan.) and carried out in SAS 9.1. The cluster analysis was complemented with regression analysis based on storm frequency, maximum chlorophyll concentration and mean river discharge.

### 3. Results

#### 3.1. Seasonal cycle

For the MAB (shaded gray area in Fig. 1), the spatially averaged monthly chlorophyll concentration revealed an annual cycle characterized by high values during fall–winter months (October–March), which decreased until it reached lowest values during the highly stratified summer months (Fig. 3). The integrated chlorophyll from October to March represented 58% of the annual chlorophyll. The fall–winter peak in chlorophyll began in the late fall and it persisted throughout the winter into early spring of the next year. The enhanced phytoplankton biomass in the fall–winter was most obvious in 2005 when there were high chlorophyll concentrations in November, which remained high until March 2006. There was significant inter-annual variability in the magnitude of the fall–winter events, for example in 2002–2003 the fall–winter chlorophyll biomass was not as elevated as in the other years of this study.

The significance of the EOF modes for the spatial and temporal variability in chlorophyll was tested following methods described by North et al. (1982). The error produced in the EOF due to the finite number of images was  $\delta\lambda \approx \lambda(2/n)^{1/2}$ , where  $\lambda$  is the eigenvalue and  $n$  is the degree of freedom. Only the first two modes were found significant. Spatial coefficients are presented in Fig. 4A and C. The color of the coefficient is directly related to the amplitude of the spatial coefficient. Temporal amplitudes of the EOF modes are presented in Fig. 5A. Therefore, the combination of the spatial and temporal variability can be obtained multiplying the spatial coefficient by the temporal amplitude. In our case, the first mode (Fig. 4A) explained 33% of the total variance, and was related with the seasonal enhanced chlorophyll in the fall–winter. It explained most of the variance between the 20 and 60 m isobaths. All the spatial coefficients were positive with the maxima found nearshore and decreasing offshore. Consequently, when they were multiplied by positive temporal amplitudes the whole field increased with respect to the chlorophyll climatology. The temporal amplitude with a 4-day interval showed high values in the fall–winter almost every year. Sometimes, there was a small

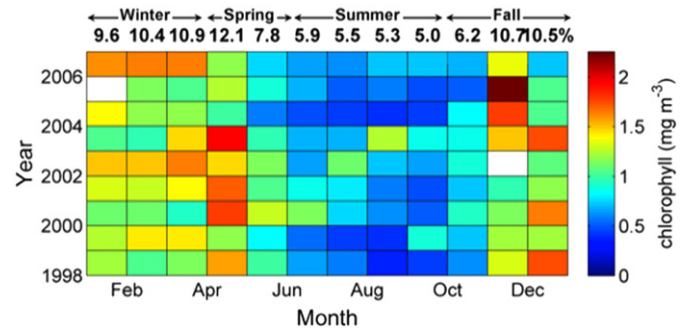


Fig. 3. Monthly mean chlorophyll ( $\text{mg m}^{-3}$ ) from January 1998 to December 2006 for MAB (shaded gray area in Fig. 1). The numbers on the top indicate the relative percentage of annual mean chlorophyll associated for each month.

increase of temporal amplitude in summer when the overall chlorophyll concentration was low ( $< 1 \text{ mg m}^{-3}$  Chl) except for the nearshore waters ( $< 30 \text{ m}$  water depth) where summer upwelling is common (Glenn et al., 2004). The spatial and temporal coefficients suggested that in the middle and outer shelf the fall–winter enhanced chlorophyll was dominant.

The satellite-derived EOF Mode 1 was consistent with the available glider observations (Fig. 6). The average sections for salinity (Fig. 6A), temperature (Fig. 6B), and optical backscatter (Fig. 6C) for the winter season showed very little vertical structure, although there was a significant cross-shore gradient. Salinity increased with distance offshore with highest values beyond 60 km from shore (Fig. 6A). Associated with the inshore lower saline waters were optical backscatter values that were 4–5 fold higher than those found in the offshore waters. The cross-shore extent of high backscatter values corresponded to the boundaries of satellite EOF Mode 1 (near 60 m isobaths) along the glider transects; however it should be noted that the optical backscatter measurements are also sensitive to the presence of sediments and plankton; however the lack of vertical structure in the glider optical data suggests that the winter satellite chlorophyll estimates are not biased by the subsurface layering in the phytoplankton populations.

The second EOF mode (Fig. 4C) explained 8% of the normalized variance and the spatial variability in mode 2 identified two different zones. The first zone had negative spatial coefficients and was located in the coastal areas within the 60 m isobath. The second zone had positive spatial coefficients located between the 80 and 150 m isobaths and extended to the MAB shelf-break front (Linder and Gawarkiewicz, 1998). Given this, the second mode applied to depths greater than 80 m and explained up to 32% of the chlorophyll local variance at those locations (Fig. 4D). The amplitude time series of the second EOF mode (Fig. 5B) generally showed positive values during spring, so when multiplied by positive spatial coefficients (yellow and red region in Fig. 4C) the whole field indicated an increase in the chlorophyll concentration over the shelf-break/slope during spring. Vice versa, the negative amplitudes multiplied by negative spatial coefficients (dark blue region in Fig. 4C) indicated that chlorophyll concentration increased such as seen in New Jersey and Long Island coastal areas during the summer months in 2001 and 2002. The increases of chlorophyll concentration in the shallow coastal area during summer might be correlated with upwelling events. Our results confirm the conclusion by Glenn et al. (2004) that the coastal regions of New Jersey in the summer of 2001 had one of the most significant upwelling events over the 9-year records (1993–2001; Moline et al., 2004), which resulted in high phytoplankton biomass. Mode 2 also exhibited enhanced chlorophyll in the fall both on the shelf and over the continental slope. The spring glider observations did exhibit

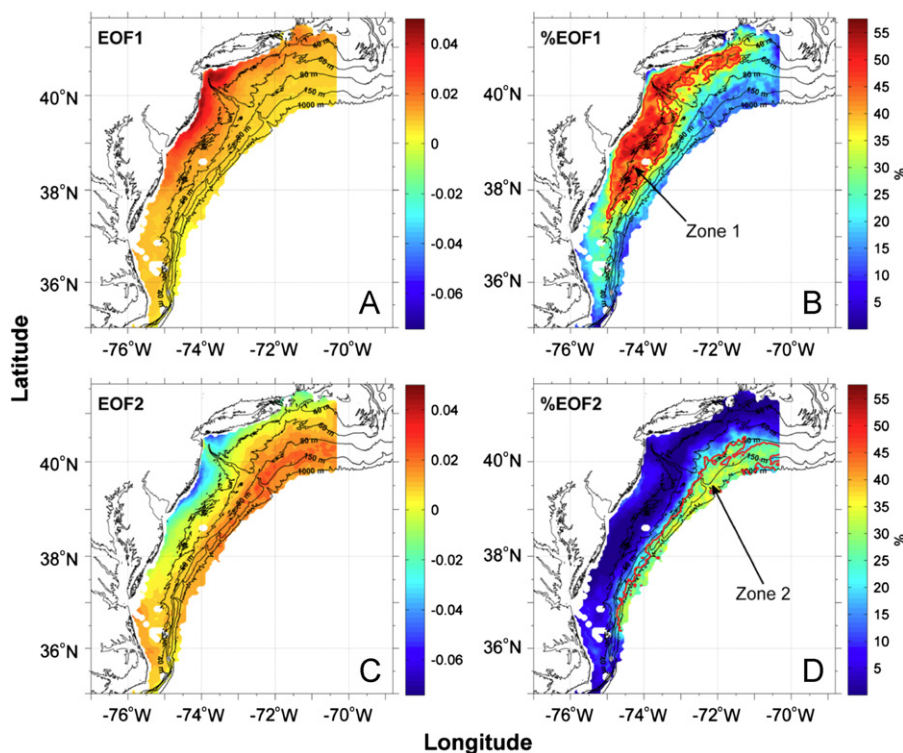


Fig. 4. The EOF modes for chlorophyll in MAB. Left panels are the first two EOF modes, right panels are percentage of the local variance explained by each mode.

enhanced particle concentrations (as detected by the optical backscatter data), both in nearshore (shallower than 30 m) and offshore (deeper than 80 m) waters (Fig. 6C, bottom panel). The enhanced particle concentrations in offshore waters were detectable during the spring, consistent with the EOF mode 2 measured by satellite. In contrast to the winter months, the spring optical data showed significant vertical heterogeneity, with the highest values found at depth. The enhanced backscatter values have been related to storm/wave/tidally driven resuspension processes (Glenn et al., 2008). The enhanced sea surface optical backscatter was associated with increased water column salinity. Low salinity water consistently had higher backscatter values in the surface (Fig. 6A, C, bottom panel).

The chlorophyll climatology in the MAB was analyzed for the two spatial zones delineated by the EOF analysis. The middle and outer shelf region (Zone 1 enclosed in Fig. 4B) where the local variance were larger than 40% identified by the first EOF mode showed mean chlorophyll concentration that ranged between 1.3 and 2.3  $\text{mg m}^{-3}$  with highest values observed in fall–winter, and lowest values observed during summer (Fig. 7A, dotted thin line). The highest chlorophyll values were inversely related to the seasonal cycle of PAR and SST, which were highest in June and August respectively. There was a two-month phase lag between PAR and SST. The measured PAR values would lead to light limitation in phytoplankton photosynthesis based on the available photosynthesis-irradiance measurements.

Six years of surface HF radar current data showed that during winter the mean surface flow on the New Jersey shelf was generally offshore and down-shelf (Fig. 8A). Based on wind data from NDBC moored buoy 44009, winter was characterized by strong northwest winds, which we define as a mean velocity of  $9.1 \text{ m s}^{-1}$  and occur 39% of the time (Gong et al., 2010). Based on the extensive spatial and temporal analysis conducted by Gong et al. (2010), we analyzed the correlations between winds and

surface transport during the winter. The cross-shelf wind and cross-shelf surface currents had strong correlations ( $R^2 > 0.7$ ) during the late fall and winter (Fig. 7A, black bold line). Since winds were predominantly from the northwest in winter, cross-shelf flow was observed during this time (Fig. 8A, Gong et al., 2010). The strong northwest winds thus increased the transport of inner shelf fresh and nutrient rich water across the middle of the shelf (Gong et al., 2010). As this occurred when chlorophyll concentrations were high (Fig. 7A, thin line with dot), we hypothesize that the cross-shelf transport of fresh water induced intermittent surface stable layer, that promoted phytoplankton growth. Moreover, the cross-shelf transport may carry coastal phytoplankton populations from the nearshore ( $< 20 \text{ m}$  depths) out across the areal extent of EOF zone 1. Therefore, the highest phytoplankton concentrations occurred when the cross-shelf currents were correlated with cross-shelf wind in the late fall and winter. Simulations using passive particle tracers support this interpretation (Gong et al., 2010).

The second EOF mode explained more than 25% of the variance at the shelf-break/slope region (zone 2 enclosed in Fig. 4D). The spatially averaged chlorophyll concentration in zone 2 exhibited a maximum chlorophyll concentration in spring that fluctuated between 0.3 and 1.5  $\text{mg m}^{-3}$  over the year. Chlorophyll concentrations began to increase as PAR began to increase. The chlorophyll concentration began to decline as SST began to increase late in spring. The second peak of chlorophyll concentration appeared in fall with a peak of 0.9  $\text{mg m}^{-3}$  as climatological means of PAR and SST began to decrease.

The six-year climatology of seasonal flow on the shelf during spring was mostly down-shelf towards the southwest (Fig. 8B). Northeast (along-shelf) winds were more common in spring and fall. The response of surface flow under northeast winds was most energetic during the transition seasons (Gong et al., 2010). Therefore, the high correlation coefficient between along-shelf wind

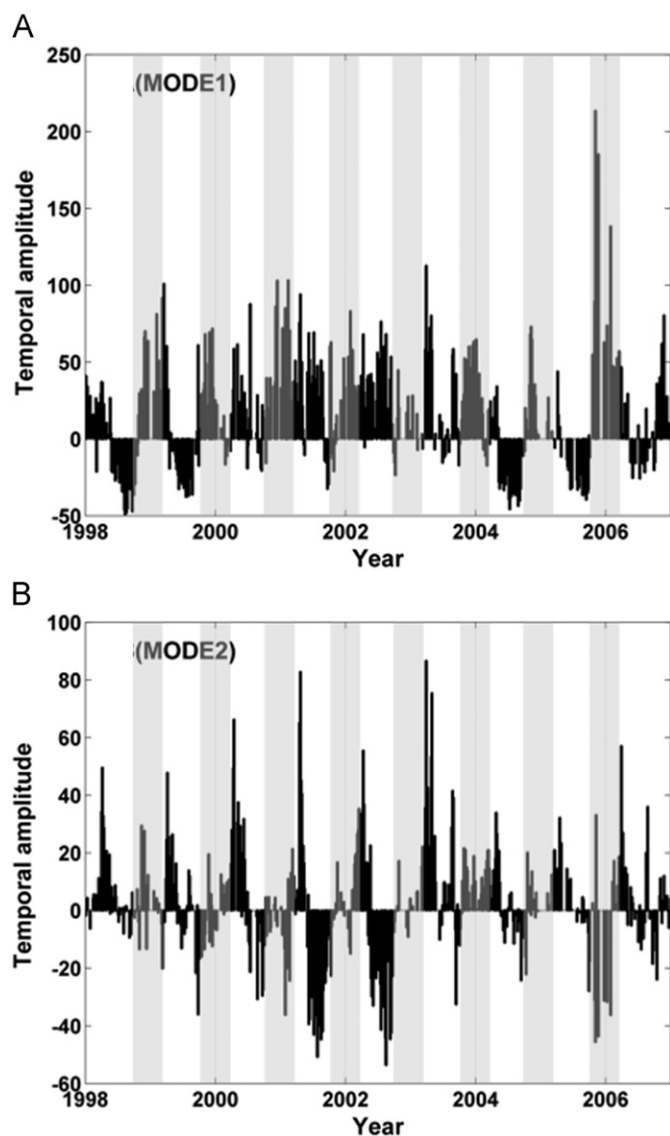


Fig. 5. Time series of the amplitude of the first two EOF modes. The gray transparent bars indicate the winter months.

and along-shelf current appeared during the transitional periods (April–May and October–November; Fig. 7B, black bold line), when the water column was stratifying in spring and as stratification was eroded in fall. The northerly winds potentially bring up shelf bottom boundary layer water through shelf-break upwelling, which is a source of nutrients and could contribute to enhanced chlorophyll in spring and fall (Siedlecki et al., 2008).

In EOF zone 2, there was another small peak of chlorophyll concentration during strongly stratified month of August. Phytoplankton growth earlier in the season would have depleted the nutrients in this region. Potentially onwelling along the slope, due to prevailing southerly wind, might have provided a source of nutrients (Siedlecki et al., 2008).

### 3.2. Mechanisms underlying the inter-annual chlorophyll variability

Over the 9-year time series, the magnitude of the enhanced chlorophyll in the fall–winter varied between 1.9 and 5.2 mg chl  $a\ m^{-3}$  (Fig. 9). One factor underlying the inter-annual variability was the presence of buoyant river plumes. In our data, the largest winter phytoplankton event occurred in 2006 and was associated with sustained high river discharge through the winter (Fig. 9).

While precipitation that year was normal, it was a warm winter and runoff was high as ice and snow formation was low. The 2006 river discharge event was observed by a Webb glider as a mid-shelf low salinity plume (as indicated by declines of 2 salinity units) in the upper mixed layer (Fig. 10B). The January 2006 winter plume was also evident as enhanced chlorophyll biomass in the SeaWiFS chlorophyll 4-day composite image from January 25th to 28th (Fig. 10A). The river plume is often transported out onto and south across the MAB under northwest wind conditions (Chant et al., 2008b). The plume can promote phytoplankton growth by stabilizing the upper water column and by transporting chlorophyll rich water from the estuary out onto the outer shelf offshore (Malone et al., 1983; Cahill et al., 2008). Additionally the river transports CDOM and non-pigmented particulate matter that can also lead to a 50–100% overestimate of chlorophyll (Harding et al., 2004). This suggests that years of high river discharge have the most biased satellite imagery. In spite of the potential satellite bias, the large river plume in 2006 contributed to the winter bloom as the river also transports extremely high concentrations of phytoplankton (Moline et al., 2008). While 2006 was the most sustained winter river discharge event, there were significant fall–winter discharge events in 1998, 2004, and 2005, which were also associated with winter blooms (Fig. 9); however, there were two years (1999–2003) where no clear relationship between river discharge and winter bloom was found suggesting other factors are also important.

Another major factor influencing the inter-annual variability in the winter bloom magnitude was the frequency of storms. Storm-induced mixing lowers the irradiance available to the phytoplankton as cells are circulated deep in the water column. The role of the storms was difficult to study as storm periods are associated with heavy cloud cover. We measured storm frequency during the months of January and February using the NOAA moored buoy 44025 where a stormy day was defined as one when wind speeds exceeded  $10\ m\ s^{-1}$ . There was a significant inverse relationship between the percent of stormy days (storm) in the winter and maximum winter chlorophyll concentration (chl  $a$ ; Fig. 11A):  $chl\ a = 4.34 - 0.05\ storm$  ( $R^2 = 0.18$ ,  $P = 0.005$ ). In the winter, even small storms are able to induce significant mixing in the water column (Dickey and Williams, 2001; Glenn et al., 2008), which can increase overall light limitation of the phytoplankton populations. We hypothesize that the storm frequency and the river discharge are important to the winter phytoplankton as both impact the stability of the water column. Including winter river discharge in the estimation of the magnitude of the chlorophyll concentration improved the regression statistics ( $chl\ a = 4.04 - 0.05\ storm + 0.000309\ river$  ( $R^2 = 0.21\%$ ,  $P = 0.02$ )).

We performed a cluster analysis to explore the relationship between winter storm frequency, chlorophyll concentration and river discharge. Results from the ten years record clustered into two groups: one was 1998, 2000, 2003, 2004, and 2005; another was 1999, 2001, 2002, 2006, and 2007. As shown in Fig. 11A, these two clusters were separated at a winter storm frequency of 27%, which we hypothesize is the threshold where mixing is sustained to decrease overall seasonal winter phytoplankton concentrations.

The spring bloom occurred at the shelf-break/slope region. The spring bloom began in late March (mean start date was March 22nd) where we defined the start of the bloom as when the chlorophyll concentrations rise 5% above that year's annual median (Siegel et al., 2002). The initiation of the spring bloom was phased around 16 days after the onset of sea surface temperature warming on the MAB. This is consistent with the hypothesis that blooms begin as the water column stratifies and phytoplankton are maintained within the euphotic zone. Given this hypothesis, the

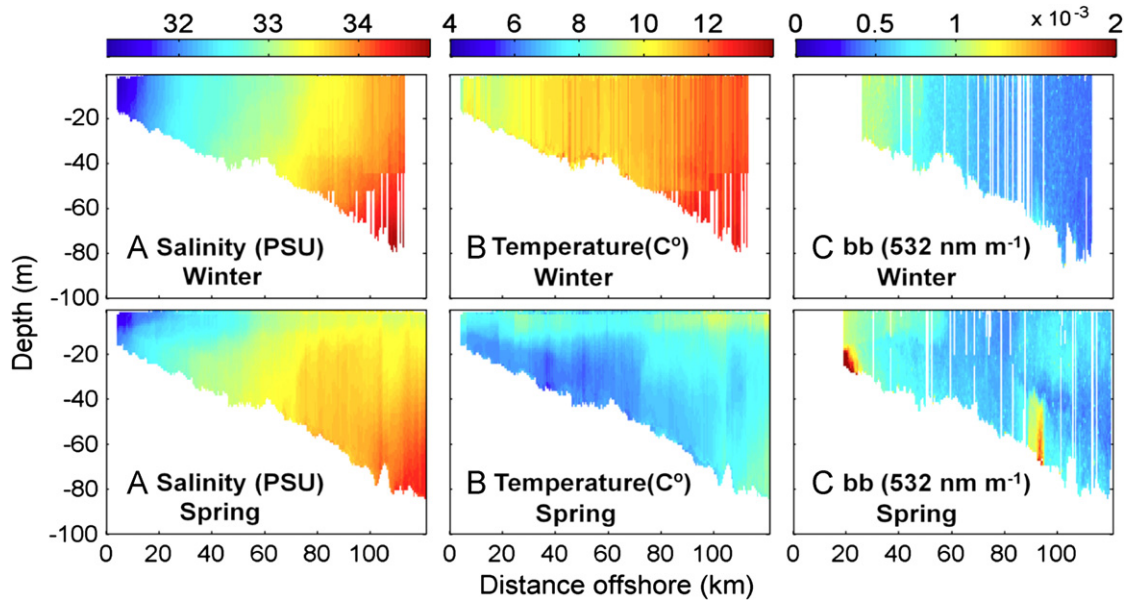


**Fig. 6.** Vertical sections of glider transect. Salinity (left), temperature (middle), and backscatter (right) collected along the Rutgers Glider Endurance line (see Fig. 1 for location; Schofield et al., 2007) during winter (top) and spring (bottom).

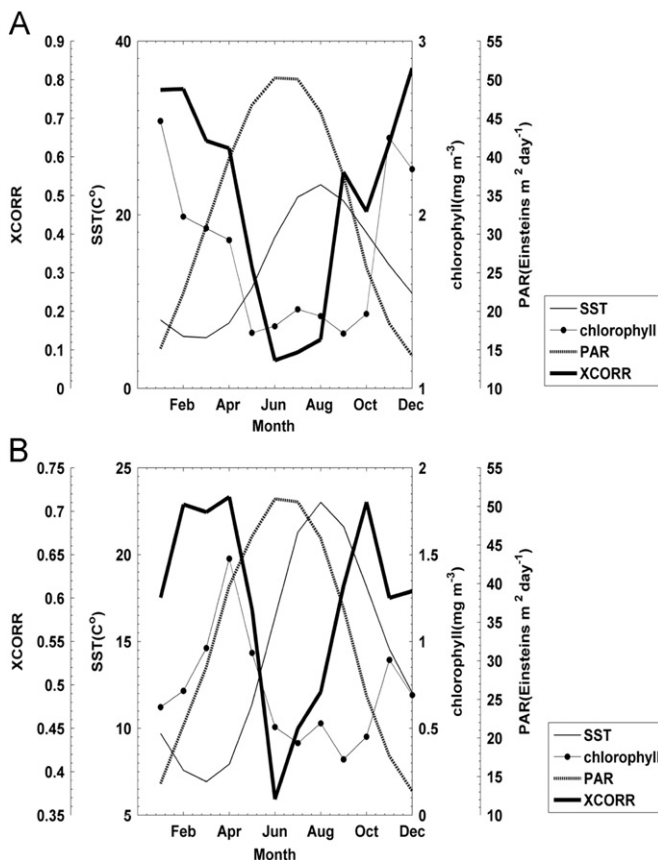


**Fig. 7.** Monthly climatology of SST (thin black line, °C), PAR (dash line, Einstein's  $\text{m}^{-2} \text{day}^{-1}$ ) and chlorophyll (thin line with dot,  $\text{mg m}^{-3}$ ) averaged over the two regions (zone 1 and zone 2 in Fig. 4) identified by the EOF analysis. Value averaged over zone 1 is shown on panel (A) together with correlation coefficient between cross-shelf wind and cross-shelf current (bold black line). Value averaged over zone 2 is shown on panel (B), together with correlation coefficient between along-shelf wind and along-shelf current. In both panels, correlation analysis used wind observations from NDBC 44009 station, and HF radar currents along the cross-shelf line, which is coincident with the glider endurance line (see Fig. 1 for location).

timing of the spring bloom should be sensitive to weather conditions in the early spring that can precondition the shelf's stratification rate. Additionally, the timing of bloom can be important to the magnitude of the spring bloom. If a bloom starts late, it may miss the 'window of opportunity' with optimum mixing and light conditions, resulting in a reduced bloom magnitude (Henson et al., 2006). Using all available data there was not a significant relationship between the magnitude of the spring bloom and number of stormy days in early spring (February–March); however, this was largely due to the spring 2003, which had a very high chlorophyll concentration despite moderate stormy conditions. Excluding 2003, there was a significant relationship ( $\text{Chl a} = 3.62 - 0.0745 \text{ storm}$ ,  $R^2 = 0.38$ ,  $P = 0.001$ , Fig. 11B).

#### 4. Discussion

Our 9-year of SeaWiFS chlorophyll data set showed two distinct zones for phytoplankton activity on the MAB. The middle and outer shelf region was associated with the recurrent winter phytoplankton blooms. The outer shelf-break/slope region was associated with the spring bloom. Although blooms in these two regions were separated in both space and time; however the magnitude of both blooms were both influenced by factors impacting water column stability.

Winter and spring phytoplankton blooms represent the major biological events in the MAB. The most recurrent and largest phytoplankton bloom occurs in winter (Ryan et al., 1999, 2001; Yoder et al., 1993, 2001, 2002), beginning in late fall and lasting through February. The winter bloom begins as the seasonal cooling erodes water column stratification, which results in the convective overturn of the water column. This process is accelerated by the passage of late fall storms (Glenn et al., 2008). The erosion of the stratification allows nutrient rich bottom waters to reach the surface alleviating nutrient limitation of phytoplankton within the euphotic zone. The spring bloom occurs on the outer shelf as seasonal warming begins to stabilize and stratify the water column. This is consistent with classical view advanced by Sverdrup (1953), and refined by Townsend et al. (1992) and

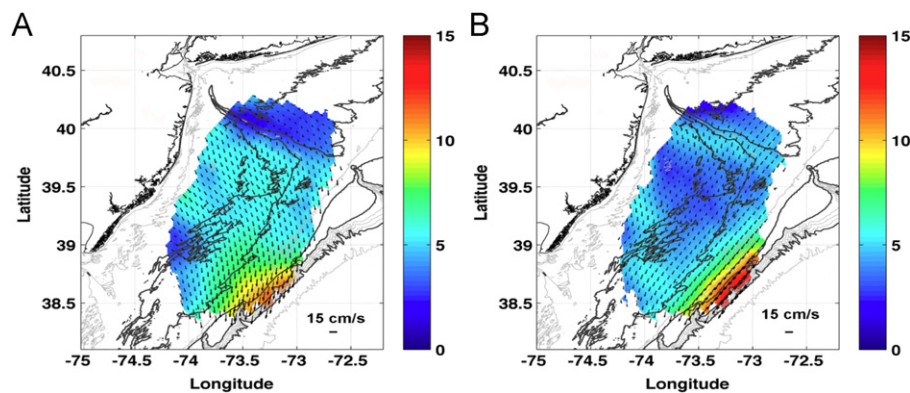


Fig. 8. Seasonal surface currents on the New Jersey Shelf ( $\text{cm s}^{-1}$ ), vectors represent the current field and the color map is the magnitude of velocity: (A) Winter (December–February) (B) Spring (March–May).

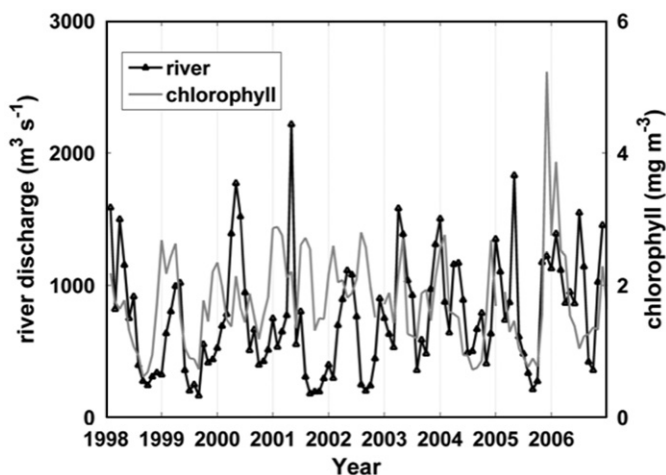


Fig. 9. Monthly and spatial averaged chlorophyll concentration (gray line) for area (zone 1 in Fig. 4(B)) depicted by the EOF mode 1 ( $\text{mg m}^{-3}$ ). The triangle marked black line represents the monthly mean river discharge in  $\text{m}^3 \text{s}^{-1}$ .

Huisman et al. (1999), that phytoplankton blooms are initiated in nutrient replete waters when vertical mixing rates are slow so that phytoplankton photosynthetic rates are sufficient to support significant phytoplankton growth. Thus light regulation is central to both the winter and spring phytoplankton blooms on the MAB.

The winter blooms over the middle and outer shelf spanned the 20–60 m isobath as delineated by EOF mode 1. We hypothesize that this depth range reflected the zone where a significant fraction of the water column had sufficient light to support phytoplankton growth. We used the satellite chlorophyll and the Hydrolight radiative transfer model to estimate the depth of the 1% light level for EOF mode 1 region. In the EOF mode 1 region, the mean water depth was 41 m and the calculated mean 1% light depth was close to 20 m; therefore 49% of the water column was above the 1% light levels (Table 1). This is significant as the winter blooms occur during the dimmest months of the year and incident light levels on the ocean surface are low. Even on the offshore side of the winter bloom at around 60 m a significant fraction of the water column resides above the 1% light level, which allows for significant photosynthesis (Falkowski and Raven, 2007). These calculations assume that the attenuation of light is only due to water and chlorophyll. In the MAB, especially when Hudson River water is present, there are other optical constituents (CDOM, detritus) that attenuate the light (Johnson et al., 2003). To assess the potential impact of the presence of Case II waters on the estimates of the 1% light depth, we combined the

available optical measurements made in the Hudson River with Hydrolight. The turbidity of the Hudson River during the LaTTE experiment decreased as the water flowed offshore; therefore we calculated the impact for two scenarios. Scenario 1 was using data collected within the Hudson shelf valley where influence of Hudson River runoff was small. Scenario 2 was the offshore Hudson River, which represented turbid conditions within the Hudson River plume on the MAB. For these waters where river water was present, the depth 1% light level decreased to 10–20 m depending on the rivers turbidity; however despite the increase in turbidity 25–50% of the water column in EOF mode 1 would remain above the 1% light level (Table 1). Thus in winter, phytoplankton appears to have sufficient light to grow when storm activity remains below the critical threshold of mixing.

The spring bloom occurred further offshore than the winter bloom and extended inshore of the MAB into shelf-break/slope area. Climatological temperature and salinity observations generally placed the foot of the front at the 80 m isobaths (Wright, 1976); however, the front location can vary by as much as 20 km (Linder et al., 2004). Therefore, the shelf-break front can possibly affect the offshore extent of the winter bloom and generally coincides with offshore extent of the spring bloom. The shelf-break and slope area range from 200 to 681 m water depths and based upon the mean satellite measured chlorophyll the 1% light depth was 33 m. This euphotic zone represents 5–17% of water column. Therefore the phytoplankton blooms occur only after the solar radiation began to increase which increases the flux of light to the surface ocean and also helps stabilizing the water column by warming the surface water. This allows the cells to overcome chronic light limitation in a deeply mixing water column (Sverdrup, 1953).

The temporal amplitude of the EOF analysis (Fig. 5) demonstrates the seasonal timing of chlorophyll blooms was consistent between years; however, there was considerable inter-annual variability in the magnitude of the winter and spring blooms. The variability in the magnitude of the blooms was associated with factors that alter the water column stability. Winters with low storm activity were characterized by having large winter phytoplankton blooms. Additionally the middle and outer shelves can be significantly influenced by the Hudson River that can deliver large buoyant plumes (Castelao et al., 2008a). These buoyant plumes stabilize the water column and transports chlorophyll from estuaries onto the shelf (Moline et al., 2008). In contrast, the spring bloom requires the shelf-break/slope water to stratify before the bloom can occur. Once the system is stratified, the pycnocline on the MAB is extremely strong and is generally not disrupted until later autumn when wind mixing and surface cooling lead to convective overturn (Biscaye et al., 1994). Given this,



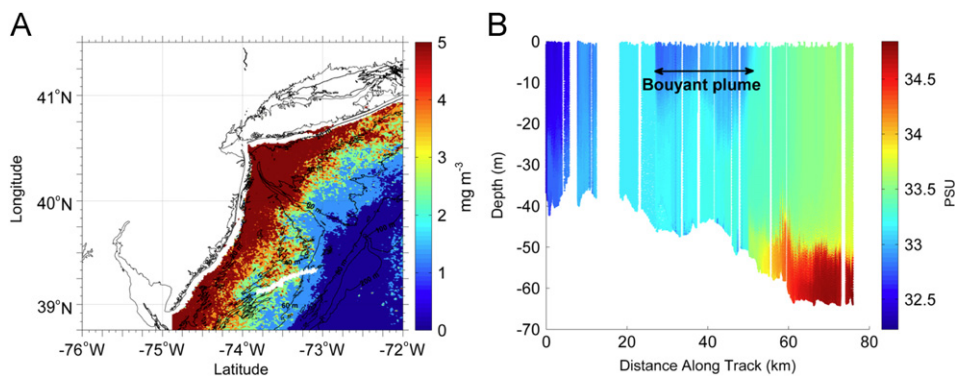


**Fig. 10.** (A) SeaWiFS chlorophyll 4-day composite image (January 25th–28th, 2006). The white line on this panel indicates the location of the glider transect. (B) Salinity cross-section measured with a glider along the transect shown in panel (A). The glider measurement is from 2006 January 18th to 23rd.

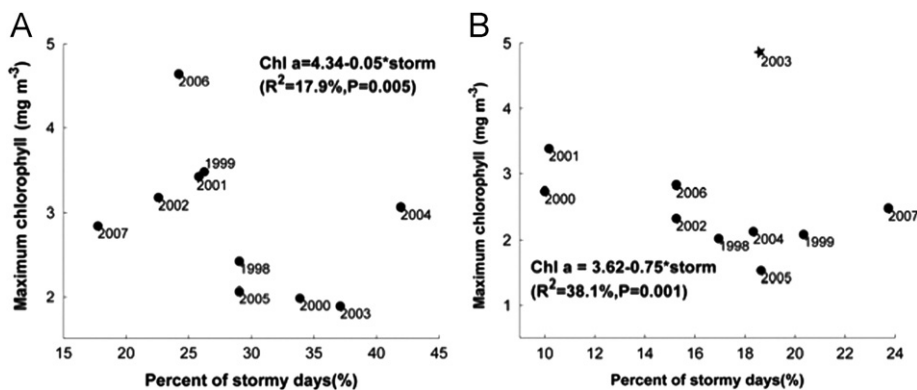


**Fig. 11.** (A) Percentage of stormy days against maximum SeaWiFS chlorophyll concentration ( $\text{mg m}^{-3}$ ) in the area depicted by EOF mode 1, (B) Percentage of stormy days against maximum SeaWiFS chlorophyll concentration ( $\text{mg m}^{-3}$ ) in area depicted by EOF mode 2. In panel (A), wind observations are from NDBC 44025 during Dec.–Jan., while in panel (B), winds are from NDBC 44014 during Feb.–Mar.; the star for 2003 marks it as an outlier.

**Table 1**

Chlorophyll ( $\text{mg m}^{-3}$ ) and light environment for the two regions defined by the EOF analysis in the MAB. For the shelf waters the 1% light depth was calculated using Hydrolight combined with optical data collected during the LaTTE experiment (Chant et al., 2008b, Moline et al., 2008).

Parameter	Shelf (zone 1)	Shelf-break (zone 2)
Mean Chl a ( $\text{mg m}^{-3}$ )	1.7	0.7
Maximum Chl a ( $\text{mg m}^{-3}$ )	4.9	2.1
Minimum Chl a ( $\text{mg m}^{-3}$ )	0.6	0.2
Mean 1% Light depth (m)	20	33
Maximum 1% Light depth (m)	12	27
Minimum 1% Light depth (m)	36	55
Mean Water Depth (m)	41	200–681 <sup>a</sup>
Percent of water column above the 1% light (%)	49	5–17
Shelf valley ac-9 data 1% light depth (m)	20	
Offshore Hudson River ac-9 data 1% light depth (m)	10	

<sup>a</sup> Much of zone 2 occurs over the continental slope. Therefore we show the depths at the inner edge of the continental slope and the mean depth of zone 2.

the factors influencing the stratification rate are the key variables to predicting the shelf-break/slope phytoplankton bloom. In the work of Lentz et al. (2003), they suggest that the direction, magnitude, and timing of spring wind stress events play an important role in inter-annual variations in stratification. For the unique year 2003, precipitation, river runoff, sea surface temperature, and air temperature were not unusual and could not account for the high spring time chlorophyll concentration.

The late winter 2003 were characterized by strong southwest winds; however, by early spring the winds shifted northeast. This resulted in predominately down-shelf and onshore transport. These northeast winds were not extremely strong in magnitude but they were sustained throughout the spring. Compared with other years, the 2003 spring had higher frequency of down-shore (53 days compared with the 11 year mean of 41 days) and towards-shore (48 days compared with the 11 year mean of 41 days) winds. Under such wind conditions, there was convergence in the bottom waters at the shelf/slope, which can result in upwelling conditions that promote phytoplankton blooms (Siedlecki et al., 2008). Therefore, while regional pre-spring wind does impact the magnitude of the spring bloom, this relationship is not particularly robust as it can be overcome by local winds. The correlation between storminess and bloom magnitude was consistent with open ocean sites (Henson et al., 2006) where storms delay the stratification of the upper ocean.

Since the MAB hydrography strongly influences the spatial and temporal patterns in satellite chlorophyll, understanding these processes is critical as the shelf water of MAB is experiencing significant changes in its temperature, salinity (Mountain, 2003). Since the 1990s, the shelf water, which is the primary water mass in the MAB, has become warmer, fresher, and more abundant than during 1977–1987. This has been correlated with transport of Scotian Shelf water and slope water and local atmospheric heat flux (Mountain, 2003). These changes are likely to influence the stratification dynamics on the MAB. The freshening of the ocean can enhance vertical stratification that has been shown to be critical to the timing and magnitude of phytoplankton blooms (Ji et al., 2007). Additionally winter wind stress has increased in

the last decade on the MAB and these changes have been associated with decadal declines in chlorophyll biomass in the fall and winter (Schofield et al., 2008). Given this, future work should focus on determining the critical thresholds between water stability and phytoplankton growth. While maximum chlorophyll concentration was affected by storm frequency and river plume, other biological factors such as nutrient concentrations or grazing may also be important. This requires new data collected for sustained periods of time to complement satellite imagery. The use of gliders as observational platforms allowed for shelf waters to be sampled frequently over long periods of time. Therefore, we recommend gliders and satellite observations be focused during the transition season and provide the basis for evaluating the relationship between stratification/destratification and the blooms in the future.

## Acknowledgments

We thank the members of the Rutgers University Coastal Ocean Observation Laboratory (RU COOL), who were responsible for the satellite, glider and CODAR operations, with particular gratitude to Jennifer Bosch and Lisa Ojanen, who helped with satellite data collection and processing. This work was supported by a grant from ONR MURI Espresso program (N000140610739) and NSF LaTTE program (OCE-0238957, OCE-0238745).

## References

- Baldacci, A., Corsini, G., Grasso, R., Manzella, G., Allen, T.J., Cipollini, P., Guymer, H.T., Snaith, M.H., 2001. A study of the Alboran sea mesoscale system by means of empirical orthogonal function decomposition of satellite data. *J. Mar. Syst.* 29, 293–311.
- Barrick, D.E., 1972. First-order theory and analysis of mf/hf/vhf scatter from the sea. *IEEE Trans. Antennas Propag.* 20, 2–10.
- Barrick, D.E., Evens, M.W., Weber, B.L., 1977. Ocean surface currents mapped by radar. *Science* 198, 138–144.
- Beardsley, R.C., Chapman, D.C., Brink, K.H., Ramp, S.R., Schlitz, R., 1985. The Nantucket Shoals flux experiment (NSFE79). Part I: a basic description of the current and temperature variability. *J. Phys. Oceanogr.* 15, 713–748.
- Biscaye, P.E., Flagg, C.N., Falkowski, P., 1994. The Shelf Edge Exchange Processes experiment, SEEP-II: an introduction to hypotheses, results and conclusions. *Deep-Sea Res.* II 41, 231–252.
- Brickley, J.P., Thomas, C.A., 2004. Satellite-measured seasonal and inter-annual chlorophyll variability in the Northeast Pacific and Coastal Gulf of Alaska. *Deep-Sea Res.* II 51, 229–245.
- Cahill, B., Schofield, O., Chant, R., Wilkin, J., Hunter, E., Glenn, S., Bissett, P., 2008. Dynamics of turbid buoyant plumes and the feedbacks on near-shore biogeochemistry and physics. *Geophys. Res. Lett.* 35, L10605.
- Campbell, J.W., 1995. The lognormal distribution as a model for bio-optical variability in the sea. *J. Geophys. Res.* 100, 13237–13254.
- Castelao, R., Schofield, O., Glenn, S., Chant, R., Kohut, J., 2008a. Cross-shelf transport of freshwater on the New Jersey shelf. *J. Geophys. Res.* 113, C07017. doi:10.1029/2007JC004241.
- Castelao, R., Glenn, S., Schofield, O., Chant, R., Wilkin, J., Kohut, J., 2008b. Seasonal evolution of hydrographic fields in the central Middle Atlantic Bight from glider observations. *Geophys. Res. Lett.* 35, L03617. doi:10.1029/2007GL032335.
- Chant, R.J., Glenn, S.M., Hunter, E., Kohut, J., Chen, R.F., Houghton, R.W., Bosch, J., Schofield, O., 2008a. Bulge Formation of a Buoyant River Outflow. *J. Geophys. Res.* 113, C01017. doi:10.1029/2007JC004100.
- Chant, R.J., Wilkin, J., Zhang, W., Choi, B.J., Hunter, E., Castelao, R., Glenn, S., Jurisa, J., Schofield, O., Houghton, R., Kohut, J., Frazer, T., Moline, M., 2008b. Dispersal of the Hudson River Plume on the New York Bight. *Oceanography* 24, 55–63.
- Crombie, D.D., 1955. Doppler spectrum of sea echo at 13.56 Mc/s. *Nature* 175, 681–682.
- Cushing, D.H., 1975. *Marine Ecology and Fisheries*. Cambridge Univ. Press, London 278 pp.
- Dickey, T.D., Williams III, A.J., 2001. Interdisciplinary ocean process studies on the New England shelf. *J. Geophys. Res.* 106, 9427–9434.
- Dutkiewicz, S., Follows, M., Marshall, J., Gregg, W.W., 2001. Interannual variability of phytoplankton abundances in the North Atlantic. *Deep Sea Res.* II 48, 2323–2344. doi:10.1016/S0967-0645(00)00178-8.
- Falkowski, P., Raven, J., 2007. *Aquatic Photosynthesis* second ed. Princeton University Press, Princeton.
- Glenn, S.M., et al., 2004. Biogeochemical impact of summertime coastal upwelling on the New Jersey Shelf. *J. Geophys. Res.* 109, C12S02. doi:10.1029/2003JC002265.
- Glenn, S.M., Jones, C., Twardowski, M., Bowers, L., Kerfoot, J., Webb, D., Schofield, O., 2008. Glider observations of sediment resuspension in a Middle Atlantic Bight fall transition storm. *Limnol. Oceanogr.* 53, 2180–2196.
- Gong, D., Kohut, J.T., Glenn, S.M., 2010. Wind driven circulation and seasonal climatology of surface current on the NJ Shelf (2002–2007). *J. Geophys. Res.* 115, C04006. doi:10.1029/2009JC005520.
- Harding, W.L., Magnusona, A., Mallonee, M.E., 2004. SeaWiFS retrievals of chlorophyll in Chesapeake Bay and the mid-Atlantic bight. *Estuarine Coastal Shelf Sci.* 62, 75–94.
- Henson, A.S., Robinson, I., Allen, J.T., Waniek, J.J., 2006. Effect of meteorological conditions on interannual variability in timing and magnitude of the spring bloom in the Irminger Basin, North Atlantic. *Deep-Sea Res.* 53, 1601–1615.
- Houghton, R., Schlitz, R., Beardsley, R., Butman, B., Chamberlin, J., 1982. The Middle Atlantic Bight cold pool: evolution of the temperature structure during Summer 1979. *J. Geophys. Res.* 12, 1019–1029.
- Huisman, J., Van, O.P., Weissing, F.J., 1999. Critical depth and critical turbulence: two different mechanisms for the development of phytoplankton blooms. *Limnol. Oceanogr.* 44, 1781–1787.
- Ji, R., Davis, C.S., Chen, C., Townsend, D.W., Mountain, D.G., Beardsley, R.C., 2007. Influence of ocean freshening on shelf phytoplankton dynamics. *Geophys. Res. Lett.* 34, L24607.
- Johnson, D.M., Miller, J., Schofield, O., 2003. Dynamics and optics of the Hudson River outflow plume. *J. Geophys. Res.* 108, 1–9.
- Kohut, J.T., Glenn, S.M., 2003. Calibration of HF radar surface current measurements using measured antenna beam patterns. *J. Atmos. Oceanic Technol.* 20, 1303–1316.
- Kohut, J.T., Glenn, S.M., Chant, R.J., 2004. Seasonal current variability on the New Jersey inner shelf. *J. Geophys. Res.* 109, C07S07. doi:10.1029/2003JC001963.
- Lentz, S., Shearman, K., Anderson, S., Plueddemann, A., Edson, J., 2003. Evolution of stratification over the New England shelf during the Coastal Mixing and Optics study, August 1996–June 1997. *J. Geophys. Res.* 108(C1), 3008. doi:10.1029/2001JC001121.
- Linder, C.A., Gawarkiewicz, G., 1998. A climatology of the shelf-break front in the Middle Atlantic Bight. *J. Geophys. Res.* 103, 18405–18423.
- Linder, C.A., Gawarkiewicz, G., Pickart, R., 2004. Seasonal characteristics of bottom boundary layer detachment at the shelfbreak front in the Middle Atlantic Bight. *J. Geophys. Res.* 109, C03049. doi:10.1029/2003JC002032.
- Longhurst, A.R., 1998. *Ecological Geography of the Sea*. Academic Press, San Diego 398 pp.
- Lorenz, E.N., 1956. Empirical orthogonal functions and statistical weather prediction. *Sci. Rep.* 1, 49 Statist. Forecasting Proj., Department Meteor., MIT.
- Malone, T.C., Hopkins, T.S., Falkowski, P.G., Whitledge, T.E., 1983. Production and transport of phytoplankton biomass over the continental shelf of the New York Bight. *Cont. Shelf Res.* 1, 305–337.
- Mobley, C.D., 1994. *Light and Water, Radiative Transfer in Natural Waters*. Academic Press, California.
- Moline, M.A., Blackwell, S., Chant, R., Oliver, M.J., Bergmann, T., Glenn, S., Schofield, O., 2004. Episodic physical forcing and the structure of phytoplankton communities in the coastal waters of New Jersey. *J. Geophys. Res.* 110, C12S05. doi:10.1029/2003JC001985.
- Moline, M.A., Frazer, T.K., Chant, R., Glenn, S., Jacoby, C.A., Reinfelder, J.R., Yost, J., Zhou, M., Schofield, O., 2008. Biological responses in a dynamic, buoyant river plume. *Oceanography* 21, 71–89.
- Mountain, D.G., 2003. Variability in the properties of Shelf Water in the Middle Atlantic Bight, 1977–1999. *J. Geophys. Res.* 108 (C1), 3014. doi:10.1029/2001JC001044.
- Navarro, G., Ruiz, J., 2006. Spatial and temporal variability of phytoplankton in the Gulf of Ca' diz through remote sensing images. *Deep-Sea Res.* II 53, 1241–1260.
- North, G.R., Bell, T.L., Cahalan, R.F., Moeng, F.J., 1982. Sampling errors in the estimation of empirical orthogonal functions. *Mon. Weather Rev.* 110, 699–706.
- O'Reilly, J., Busch, D., 1984. Phytoplankton primary production on the north-west Atlantic Shelf. *Rapports et Proces-Verbaux des Reunions Conseil International pour l'Exploration de la Mer* 183, 255–268.
- Pawlowicz, R., Beardsley, R.C., Lentz, S.J., 2002. Classical tidal harmonic analysis including error estimates in MATLAB using T TIDE. *Comput. Geosci.* 28, 929–937.
- Riley, G.A., 1946. Factors controlling phytoplankton populations on Georges Bank. *J. Mar. Res.* 6, 54–73.
- Riley, G.A., 1947. Seasonal fluctuations of the phytoplankton population in New England coastal waters. *J. Mar. Res.* 6, 114–125.
- Ryan, J.P., Yoder, J.A., Cornillon, P.C., 1999. Enhanced chlorophyll at the shelfbreak of the Mid-Atlantic Bight and Georges Bank during the Spring Transition. *Limnol. Oceanogr.* 44, 1–11.
- Ryan, J.P., Yoder, J.A., Townsend, D.W., 2001. Influence of a Gulf Stream warm-core ring on water mass and chlorophyll distributions along the southern flank of Georges Bank. *Deep-Sea Res.* II 48, 159–178.
- Ryther, J.H., Yentsch, C.S., 1958. Primary production of continental shelf waters off New York. *Limnol. Oceanogr.* 3, 327–335.
- Schofield, O., Bergmann, T., Oliver, M., Irwin, A., Kirkpatrick, G., Bissett, W.P., Orrico, C., Moline, M.A., 2004. Inverting inherent optical signatures in the nearshore coastal waters at the Long Term Ecosystem Observatory. *J. Geophys. Res.* 109, C12S04. doi:10.1029/2003JC002071.
- Schofield, O., et al., 2007. Slocum gliders: robust and ready. *J. Field Robotics* 24, 1–14. doi:10.1009/rob.202000.

- Schofield, O., Chant, R., Cahill, B., Castelao, R., Gong, D., Kohut, J., Montes-Hugo, M., Ramanduri, R., Xu, Y., Glenn, S., 2008. Seasonal forcing of primary productivity on broad continental shelves. *Oceanography* 21, 108–117.
- Schofield, O., Chant, R., Hunter, E., Moline M.A., Reinfelder, J., Glenn, S.M., Frazer, T. Optical transformations in a turbid buoyant plume on the Mid-Atlantic Bight. Continental Shelf Research, submitted for publication.
- Siedlecki, S.A., Mahadevan, A., Archer, D., 2008. The Role of Shelf Break Upwelling Along the East Coast of the US in the Coastal Carbon Cycle: A Model's Tale. American Geophysical Union, Fall Meeting 2008, poster #OS53C-1322.
- Siegel, D.A., Doney, S.C., Yoder, J.A., 2002. The North Atlantic spring phytoplankton bloom and Sverdrup's critical depth hypothesis. *Science* 296, 730–733.
- Stewart, R.H., Joy, J.W., 1974. HF radio measurement of surface currents. *Deep-Sea Res.* 21, 1039–1049.
- Stramska, M., Dickey, T., 1994. Modeling phytoplankton dynamics in the northeast Atlantic during the initiation of the spring bloom. *J. Geophys. Res.* 99, 10,241–10,253.
- Sverdrup, H.U., 1953. On conditions for the vernal blooming of phytoplankton. *J. Cons. Perm. Int. Explor. Mer.* 18, 287–295.
- Townsend, D.W., Keller, M.D., Sieracki, M.E., Ackleson, S.G., 1992. Spring phytoplankton blooms in the absence of vertical water column stratification. *Nature* 360, 59–62.
- Townsend, D.W., Cammen, L.M., Holligan, P.M., Campbell, D.E., Pettigrew, N.R., 1994. Causes and consequences of variability in the timing of spring phytoplankton blooms. *Deep-Sea Res. I* 41, 747–765.
- Ueyama, R., Monger, B.C., 2005. Wind-induced modulation of seasonal phytoplankton blooms in the North Atlantic derived from satellite observations. *Limnol. Oceanogr.* 50, 1820–1829.
- Ward, J.H., 1963. Hierarchical grouping to optimize an objective function. *J. Am. Statist. Assoc.* 58, 236–244.
- Wright, W.R., 1976. The limits of shelf water south of Cape Cod, 1941–1972. *J. Mar. Res.* 34, 1–14.
- Wirick, C.D., 1994. Exchange of phytoplankton across the continental shelf-slope boundary of the Middle Atlantic Bight during spring 1988. *Deep-Sea Res. II* 41, 391–410.
- Yoder, J.A., McClain, C.R., Feldman, G.C., Esaias, W.E., 1993. Annual cycles of phytoplankton chlorophyll concentrations in the global ocean: a satellite view. *Global Biogeochem. Cycles* 7, 181–194.
- Yoder, J.A., O'Reilly, J.E., Barnard, A.H., Moore, T.S., Ruhsam, C.M., 2001. Variability in coastal zone color scanner (CZCS) Chlorophyll imagery of ocean margin waters off the US East Coast. *Cont. Shelf Res.* 21, 1191–1218.
- Yoder, J.A., Schollaert, S.E., O'Reilly, J.E., 2002. Climatological Phytoplankton Chlorophyll and Sea Surface Temperature Patterns in Continental Shelf and Slope Waters off the Northeast U.S. Coast. *Limnol. Oceanogr.* 3, 672–682.